Revista Brasileira de Meteorologia, **v.26**, **n.4**, 529 - 540, 2011

ATMOSPHERIC CO_2 BUDGET OVER THE AMAZON BASIN:THE ROLE OF CONVECTIVE SYSTEMS

VALDIR HERRMANN[1] AND SAULO RIBEIRO DE FREITAS[2]

[1]Climatempo Meteorology, São Paulo, SP, Brazil, valdir@climatempo.com.br.
[2]National Institute fot Space Research, Center for Weather Prediction and Climate Studies, Cachoeira Paulista, SP, Brazil,

saulo.freitas@cptec.inpe.br.

Received April 2010 – Accepted February 2011

ABSTRACT

This work studies the atmospheric CO_2 budget in the Amazon basin, focusing on the role of shallow and deep convective systems. The vertical redistribution of CO_2 is numerically simulated using an Eulerian transport model coupled to the Brazilian developments on the Regional Atmospheric Modeling System (BRAMS). The transport model includes grid-scale advection, diffusion in the PBL (Planetary Boundary Layer) and convective transport by sub-grid shallow and deep moist convection. In the simulation, the mass conservation equation is solved for six tracers, including or not the shallow and deep moist convection terms. The rectifier effect is also showed through simulation of the transport to the free troposphere of PBL air masses with low CO_2 concentrations due to assimilation by vegetation during the afternoon, when both CO_2 fixation and convection are at their peak. The model is applied to simulate July 2001 with a 30 km grid resolution covering the northwest part of South America. We compare the model results with airborne CO_2 observations collected in the Amazon basin during the 2001 CLAIRE field campaign.
Keywords: carbon budget, Amazon basin, convective transport, CO2 flux

RESUMO: BALANÇO DE CO_2 NA ATMOSFERA DA BACIA AMAZÔNICA: O PAPEL DOS SISTEMAS CONVECTIVOS

Este trabalho apresenta um estudo do balanço de CO_2 na atmosfera da bacia Amazônica, enfocando o papel dos sistemas convectivos rasos e profundos. A redistribuição vertical de CO_2 é simulada numericamente usando um modelo de transporte Euleriano acoplado ao modelo atmosférico BRAMS (Brazilian developments on the Regional Atmospheric Modeling System). O modelo de transporte inclui o termo de advecção, associado ao transporte resolvido, além dos termos de transporte, não resolvidos como dif'usão turbulenta na CLP (Camada Limite Planetária), e transporte convectivo, associado a cumulus rasos e profundos. Na simulação utilizam-se seis traçadores, onde a equação da conservação da massa é resolvida incluindo ou não o termo convectivo profundo ou o termo convectivo raso. O efeito retificador é descrito na simulação numérica através do transporte para a troposfera livre de massas de ar da CLP com baixas concentrações de CO_2, devido à atividade de assimilação realizada pela vegetação no período diurno, quando os dois processos, fixação e atividade convectiva estão no ápice. A simulação foi realizada para o mês de julho de 2001, com uma resolução de 30 km na grade, cobrindo a porção noroeste da América do Sul. Comparações dos resultados do modelo com dados de CO_2 , observados na bacia Amazônica durante o experimento CLAIRE – 2001, também são mostradas.
Palavras-Chave: Balanço de Carbono, Amazônia, Transporte Convectivo, Fluxos de CO2.

1. INTRODUCTION

The atmosphere is composed of a mixture of gases and aerosols, which interact with solar and terrestrial radiation. Solar radiation is absorbed, reflected, and scattered in a complex combination of interactions with the atmosphere and ground surface. Part of the incident shortwave radiation is absorbed by the Earth's surface and reemitted in the infrared (longwave) range. Chemical species such as carbon dioxide (CO_2), methane (CH_4), nitrous oxide (N_2O), water vapor (H_2O), and chlorofluorocarbons (CFCs), among others, absorb long wave radiation emitted by the Earth's surface and atmosphere, producing the so-called "greenhouse effect," responsible for life on Earth. In the absence of these gases, the Earth's temperature would be approximately 30°C cooler, compromising all existing ecosystems. Thus, the study of the atmospheric budget of these gases is crucial for understanding climate change on Earth.

At the global level, the most important biosphere-atmosphere interactions are the transfers of energy, water and carbon. According to Malhi et al. (1998), the magnitude of these processes varies by biome, with forests recognized as a major CO_2 sink. Forests cover around 12% of the Earth's surface and are estimated to contain 40% of the carbon in the terrestrial biosphere (Whittaker and Likens, 1975; Taylor and Lloyd, 1992). Carbon is absorbed by the biosphere through photosynthesis and produced by the respiration of plants, animals, microbes, etc.

Anthropogenic sources, such as fossil fuel and biomass burning, also contribute to the increase of CO_2 in the atmosphere. Andreae et al. (1988) showed that CO_2 emissions from biomass burning occur primarily in tropical and subtropical regions during the dry season (June to October in the Southern Hemisphere). Emissions of CH_4 and nitrous oxide (NO_x) also contribute to the greenhouse effect. Methane emissions are on the order of 1% of the quantity of CO_2; however, the radiative effect of a molecule of CH_4 is 25 times greater than that of CO_2 (Houghton, 1990). Agricultural biomass burning emissions of CO_2 can be reincorporated into vegetation during the annual growth cycle. However, this is not possible in deforested areas because regrowth, if it occurs, takes a long time (on a scale of several decades), leading to a net emission of CO_2 to the atmosphere. In the presence of solar radiation and high concentrations of NO_x, the oxidation of CO and hydrocarbons results in the formation of ozone (O_3). The combination of thousands of fires during the dry season produces an extensive plume affecting the regional chemical composition and radiative balance of the atmosphere in South America (Freitas et al, 2005).

At the local scale, where inorganic carbon (CO_2) is absorbed by vegetation and transformed into an organic component, the exchange of carbon between the Earth's surface and atmosphere is controlled by solar radiation. Thus, the diurnal solar cycle, causing variations in the photosynthesis cycle, is the principal factor in the assimilation of atmospheric carbon. The flux of CO_2 emitted from the surface to the atmosphere is the difference between the assimilation of CO_2 by plants and the emission from soil and plants. During the day, the presence of sunlight causes assimilation and emission to occur simultaneously. At night, assimilation is nonexistent due to the absence of light, and only respiration is maintained. Thus, under calm nocturnal conditions with strong atmospheric stability, CO_2 accumulates in the lower troposphere. Consequently, high concentrations of carbon are observed in the early morning hours. Throughout the day, the carbon concentration decreases due to photosynthesis and the deepening of the mixing layer, but rise again in the following night.

This work consists of a numerical study of the atmospheric CO_2 budget over the Amazon basin, focusing on the role of the "rectifier" effect of convective systems operating in the region. This effect consists of the tendency of convective systems to transport air masses with low CO_2 concentrations from the PBL to the free troposphere during the afternoon, when both convective activity and CO_2 assimilation by vegetation are at their peaks. Additionally, a shallow cumulus parameterization is used to evaluate the role of these systems and their interaction with deep convection in the vertical redistribution of CO_2.

This paper is organized as follows: the methodology is presented in Section 2, with numerical results and discussion in Section 3. A summary and conclusions are presented in Section 4.

2. MATERIALS AND METHODS

The CO_2 budget is studied through numerical atmospheric modeling using the Coupled Aerosol and Tracer Transport model to the Brazilian developments on the Regional Atmospheric Modeling System (CATT-BRAMS, Freitas et al, 2005, 2009). CATT is an in-line Eulerian transport model, which permits following the transport of tracers simultaneously with the evolution of the atmospheric state. The Regional Atmospheric Modeling System (RAMS) is a numerical code developed at Colorado State University (USA) to produce diagnostic and prognostic simulations of the atmospheric state (Walko et al., 2000). The model was constructed from the complete set of primitive equations that govern atmospheric motions, and includes parameterizations of the diverse physical processes present in these equations. It is possible to activate and deactivate the variety of options and parameterizations present in the code, and to define the grid positioning, domain, and resolution depending on the needs of the study being developed. BRAMS has various improvements, including a new shallow and deep cumulus scheme, based on the mass flux formulation

and with various types of closures (Grell, 1993; Grell e Devenyi, 2002), and the coupling of the transport of tracers associated with these systems.

2.1 The transport model

The transport model follows the Eulerian approach and is executed simultaneously (in-line) with the atmospheric model. It solves the following mass conservation equation, written in the tendency form:

$$\frac{\partial s}{\partial t} = \left(\frac{\partial s}{\partial t}\right)_{adv} + \left(\frac{\partial s}{\partial t}\right)_{\substack{PBL \\ turb}} + \left(\frac{\partial s}{\partial t}\right)_{\substack{deep \\ conv}} + \left(\frac{\partial s}{\partial t}\right)_{\substack{shallow \\ conv}} + F \quad (1)$$

where s (= ρ/ρ_{air}) is the tracer mixing ratio, and adv, PBL turb, deep conv and shal conv refer to the terms of advective transport by mean wind, turbulent transport in the PBL, sub-grid transport by precipitating convective systems, and sub-grid transport by shallow convection, respectively. F refers to the CO_2 source/sink term associated with biogenic activity in the Amazonian ecosystem. In the time period of the simulation, biomass burning is not a relevant CO_2 source. Additionally, urban pollution in this area has a minor impact and will be disregarded in this study. The advection and PBL diffusive transport terms are calculated using the RAMS parameterizations. The horizontal diffusion is based on the formulation of Smagorinsky (1963). Vertical diffusion is parameterized according to the scheme of Mellor and Yamada (1974). Advection is solved with a second-order forward upstream scheme (Tremback *et al.* 1987).

The convective transport of tracers is based on the Grell convection scheme (Grell, 1993; Grell e Devenyi, 2002). The tendency term associated with deep convection is given by:

$$\left(\frac{\partial s}{\partial t}\right)_{\substack{deep \\ conv}} = \frac{m_b}{\rho_0}\left[\delta_u \eta_u \left(s_u - \tilde{s}\right) + \varepsilon \delta_d \eta_d \left(s_d - \tilde{s}\right) + \tilde{\eta}\frac{\partial \tilde{s}}{\partial z}\right], \quad (2)$$

where m_b is the mass flux of updrafts in the cloud base, ρ_0 is the air density, δ is the mass detrainment rate, η is the normalized mass flux, the indices u and d indicate updrafts and downdrafts, respectively, and z is cartesian height. The term ε represents the ratio of updraft and downdraft mass fluxes, and $\tilde{\eta}$ is the environment normalized mass flux. These parameters are estimated by the convection scheme. s_u, s_d and $\tilde{s}$ represent the tracer mixing ratios in updrafts, downdrafts, and the background, respectively. Thus, in this equation the first right-hand term refers to the mass removal by deep convective updrafts, the second to mass removal by downdrafts, and the third to background advection (subsidence). In this context, updrafts transport material from the PBL to the upper troposphere, while downdrafts bring material into the PBL from the middle troposphere.

The shallow non-precipitating sub-grid transport term follows the same formulation, disregarding the occurrence of downdrafts:

$$\left(\frac{\partial s}{\partial t}\right)_{\substack{shallow \\ conv}} = \frac{m_b}{\rho_0}\left[\delta_u \eta_u \left(s_u - \tilde{s}\right) + \tilde{\eta}\frac{\partial \tilde{s}}{\partial z}\right] \quad (3)$$

with the first right-hand term of Equation 3 associated with mass detrainment rate of the updrafts and the second with environmental advection (subsidence). Here shallow cumulus act only to ventilate material from the PBL into the lower troposphere. For more details, see Freitas et al., 2005.

2.2 Parameterization of the CO_2 source/sink term

The CO_2 source/sink term (F) associated with biogenic fluxes was parameterized following two different approaches:

2.2.1 Cosinusoidal Formulation

In this formulation, the F_{CO_2} term is expressed simply in the following form:

$$F_{CO_2} = R - P, \quad (4)$$

where R represents the flux associated with respiration and P with assimilation. The term R is considered to be constant with time, depending only on the vegetation type. The spatial domain was divided into three dominant biomes with values for R (μmol m^{-2} s^{-1}) equal to 5, 5, and 2.8 for forest, pasture, and savanna (Lu et al. 2005, Miranda et al 1996), respectively. The assimilation during the diurnal period was given by a cosinusoidal function, with the maximum value depending on the biome. The expression is given by:

$$P(t) = \begin{cases} 0 \rightarrow \text{night time} \\ P_0 \cos\left(\dfrac{\pi t}{12}\right) \rightarrow \text{day time} \end{cases} \quad (5)$$

where t represents the local time (LT) and P_0 the maximum assimilation rate (in μmol m^{-2} s^{-1}). Here night and day time refer to the time period comprised between 18 PM to 6 AM and 6 AM to 18 PM, respectively. As with respiration, the maximum assimilation rate P_0 is spatially distributed using a vegetation type map, with the following values: 25, 20 and 15 for forest, pasture, and savanna (Lu et al. 2005, Miranda et al 1996), respectively.

2.2.2 Formulation obtained from net radiation correlation

In this section, the fluxes are parameterized using observational data obtained from micrometeorological towers. For forested areas, data was used from the experiment "CO_2

Budget and Rectification Airborne study" (COBRA, http://www-as.harvard.edu:16080/chemistry/cobra) conducted in April 2001 in the Tapajós National Forest (FNT), located around 50 km to the south of Santarém in the State of Pará. In this region, the forest cover an area of approximately 600,000 hectares, with an average canopy height of 40 m, and is located between the Tapajós River and the Santarém-Cuiabá highway. The seasonal rainfall characteristics are influenced by the migration of the Intertropical Convergence Zone (ITCZ), bringing the largest quantity of rain from February to April. Less rainfall is observed during the months of September to November, constituting the driest period in the region.

Using a tower with a height of 65 m and automatically installed instrumentation, micrometeorological measurements were made using the eddy correlation method, with continuous fluxes measurements of momentum, CO_2 (described in terms of net ecosystem exchange, NEE), and H_2O. Simultaneously, measurements were made of net radiation and other meteorological variables, such as temperature, humidity and wind.

In this case, the CO_2 flux was parameterized using the observed correlation between the carbon flux (F_{CO_2}) and the net surface radiative flux ($\Re_{net}$):

$$F_{CO_2} = a + b\Re_{net}, \qquad (6)$$

Figure 1 shows the resulting correlation curve, with a coefficient of determination equal to 0.95 for the forest site. The correlation coefficients ***a*** and ***b*** were 6.71 and -0.0375, respectively. This correlation was obtained by applying a minimum friction velocity criterion of (u*) equal to 0.2 m s^{-1} and thus eliminating cases of extreme atmospheric stability that can introduce an underestimation in the flux measurements (Saleska et al. 2003). Comparison of the average hourly fluxes with and without the filter associated with u* show significant differences during the nocturnal period only, as one would expect, and is described in Herrmann (2004). Table 1

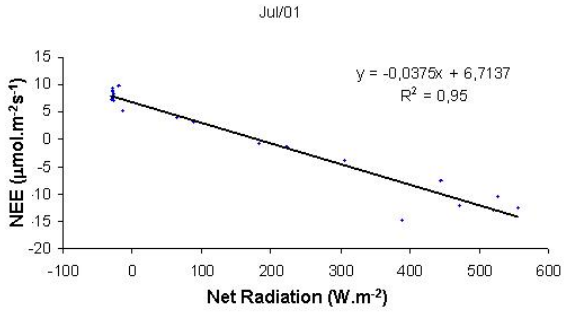

Figure 1 - Correlation between CO2 flux and surface net radiation (forest site) for July 2001.

Table 1 - Parameterization of net CO2 flux based on data obtained from flux towers data.

$F_{CO_2} = a + bR_{NET}$ (µmol $m^{-2}s^{-1}$)		
	a	***b***
Forest	**6,71**	**-0,0375**
Pasture	**4,53**	**-0,0375**

summarizes the estimated parameters for the forest and pasture (Fazenda Nossa Senhora, located in the municipality of Ouro Preto do Oeste in Rondônia state) sites. For the pasture site, the coefficient of determination is equal to 0.93. Using the model's vegetation map and the net radiation simulated at each time step, the CO_2 flux from the atmosphere to the surface is spatially and temporally estimated using Equation 6.

The CO_2 flux at water surfaces was parameterized simply as a sink and constant in time according to the work of Takahashi et al. (1999) and Lixin et al. (2005). The values used were 0.05 for oceans and 5 µmol/ (m^2s) for lakes and continental rivers.

As each model grid cell could simultaneously contain portions of land and water, the effective flux in the cell is given by:

$$F_{CO_2} = fF_{CO_{2\,land}} + (1-f)F_{CO_{2\,water}}, \qquad (7)$$

with f the land fraction in the grid cell.

2.3 Use of simultaneous tracers for studying isolated processes

In order to study the role of convective systems in the transport of CO_2 in the atmosphere, focusing principally on the 'rectifier' effect, various tracers are simulated simultaneously using the same atmospheric model physics and dynamics. Here, five different tracers are simulated by solving the continuity equation (Equation 1), including various combinations of processes. Table 2 summarizes the considered processes. For example, the CO_2[1] and CO_2[5] tracers are simulated with all the relevant transport processes, but varying the formulation of the source/sink term. The CO_2[2] tracer is not transported by shallow convection and CO_2[3] is not affected by deep precipitating convection, while CO_2[4] is only advected and diffused inside the PBL

2.4 Model configuration

Numerical modeling was conducted with the goal of simulating the CO_2 flux behavior over part of the Amazon basin. During this process, it was possible to conduct a numerical study of the vertical CO_2 profile, and of how this gas is transported from the PBL to the free troposphere in the different atmospheric systems present in the analyzed region. The chosen study period

Table 2 - The five different CO2 tracers with their respective terms from the CO2 transport equation. Checkmarks indicate the terms that were considered in each simulation. *Use of the source parameterization (correlation between NEE and net radiation).

Tracer	Advec	PBL turb	Deep Conv	Shal Conv	***F*** (sources)
CO_2[1]	✓	✓	✓	✓	✓ *
CO_2[2]	✓	✓	✓		✓ *
CO_2[3]	✓	✓		✓	✓ *
CO_2[4]	✓	✓			✓ *
CO_2[5]	✓	✓	✓	✓	✓

was July 7 – 20, 2001, when the field campaign CLAIRE-LBA (Cooperative LBA Airborne Regional Experiment, Lloyd et al., 2007) took place near Manaus city. The model was initialized at 12:00 UTC on the 7th of July 2001 and integrated for 13 days using a time step of 50 seconds. It was configured with a spatial resolution of 30 km covering the Amazon basin (185 grid points in longitude and 78 in latitude). The vertical spatial resolution varied between 80 and 850 meters, with 40 atmospheric levels and model top at approximately 22 km height. The soil model had 7 layers with a maximum depth of 5 meters. Atmospheric analyses from the global model COLA/CPTEC were used as initial and boundary conditions for the model atmospheric fields. The soil moisture was initialized with data described in Gevaerd and Freitas (2006), which utilizes antecedent precipitation obtained from remote sensing together with an off-line hydrological model in order to estimate the stored soil water content. The vegetation map was updated with data provided by the project PROVEG (Sestini et al., 2003) with 1km spatial resolution. For CO_2, all tracers were initialized homogeneously in the horizontal direction based on the vertical profile observed on the 7th by an instrumented airplane (Figure 2), above the maximum altitude reached by the air plane, typically 4 km, a constant value of 366 ppmv was set.

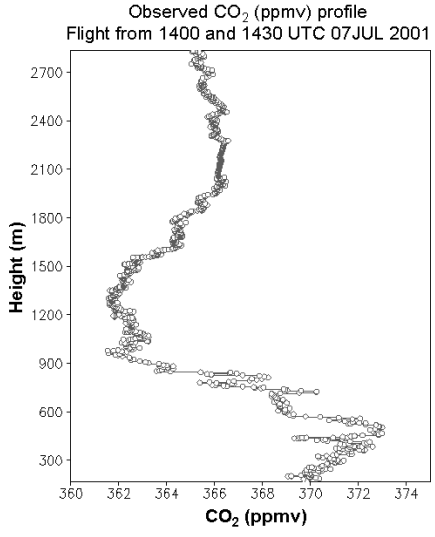

Figure 2 - Vertical CO2 profile obtained during the CLAIRE-LBA 2001 field campaign, used to initialize CO2 in the numerical simulation.

3. RESULTS AND DISCUSSION

The observed profile shows characteristics typical of the CO_2 distribution during morning periods. Near the surface, there is an excess of CO_2 relative to the free troposphere due to the accumulation of CO_2 generated during nocturnal respiration. Between 900 and 1500 meters, there is a CO_2 deficit relative to the free troposphere, indicating the presence of a residual layer associated with the mixing layer developed during the previous day. Between 1500 and 2000 meters, the CO_2 distribution shows a transition between 362 and 366 ppm. Between 2000 meters and the maximum height of the observed profile, the CO_2 mixing ratio is practically constant, with a value of 366 ppm. In the absence of a boundary condition for CO_2, a constant flux condition is assumed when directed inward and variable when directed outward.

Two physical parameterizations relevant to this study included a radiation parameterization based on Chen and Cotton (1983, referenced CC1983) that includes interaction between short and long wave radiation and liquid water content, and a shallow and deep convective parameterization based on Grell and Devenyi (2002). For the flux parameterization described in Section 2.2.2, the net surface radiation necessary for estimating the CO_2 flux is obtained from the numerical simulation using the CC1983 scheme, instead of from observations. This is necessary in order to maintain the consistency between the CO_2 fluxes and dynamics simulated by the model. Figure 3b shows a comparison between the observed $\Re_{net}$ and that simulated by the model in the grid cell that contains the TNF observational site. The model overestimates the radiation by 15 to 30% relative to the observed values for the diurnal period during the entire simulation period. This overestimation is attributed to the inability of the model to capture the variability of cloud cover that occurred over the TNF during this period. A comparison of the simulated and observed CO_2 fluxes is shown in Figure 3a. The NEE observed during the period from 7 – 20 June is shown in black. The nocturnal respiration varied between approximately 2 and 15 ì mol $m^{-2}s^{-1}$. The simulated fluxes were

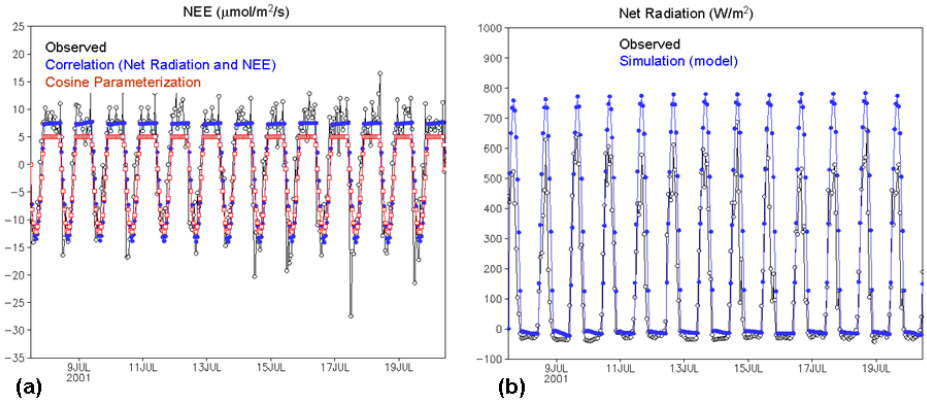

Figure 3 - For July 9 – 10, 2001, (a) comparison of parameterization based on the correlation between CO2 flux and Rnet, cosinusoidal parameterization of CO2 flux, and observed flux, and (b) comparison of observed and modeled Rnet.

approximately constant with values from 5 to 7.5 ì mol $m^{-2}s^{-1}$ for the cosinusoidal formulation (in red) and that obtained through correlation (in blue), respectively. From visual inspection, it is apparent that the correlation method represents well the observed nocturnal average. During the diurnal period, both formulations exhibit similar behavior. During the first week, both compare reasonably well with observations. However, during the second week, extreme values of NEE around 30 ì mol $m^{-2}s^{-1}$ were observed during short time intervals. These extremes were not captured by the two formulations. In general, the second formulation compared more favorably with observations.

Figure 4 shows a comparison of four vertical profiles simulated using the two CO_2 flux parameterizations with observations for July 7, 10, 14, and 17, in the morning and late afternoon. The red line represents the CO_2 concentrations measured by aircraft from the surface to a height of approximately 3000 m. Complex structures associated with turbulent transport are noted principally inside the PBL. Simulated values utilizing the cosinusoidal and correlational parameterizations are shown in blue and black, respectively. The simulated values are compared with the spatial average in the aircraft sampling area, located approximately between the longitudes 60º30'W and 59º30'W and the latitudes 3º30'S and 2º30'S. Figure 4a shows the profiles 2 hours after the beginning of the simulation, essentially representing the initial condition. Figure 4b corresponds to 2000 UTC (1600 LT) and show typical conditions for the afternoon, with a well-developed convective boundary layer with a depth of around 1200 meters, typical for the Amazon rainforest. Both profiles exhibit a CO_2 deficit relative to the free troposphere due to the flux of CO_2 assimilated by the forest. Clearly, the results for the CO_2[1] tracer are significantly better than those of CO_2[5]. It is noted that due to the spatial resolution and the simplified PBL numerical formulations in the model, it is not possible to capture all the details of the observations. Even so, the simulated profile represents well the average measured value of CO_2. For the CO_2[5] tracer, there is an mean difference of around 6 ppm relative to the observations. Since the intensity of the diurnal flux in this case is comparable with that of the CO_2[1] tracer (see Figure 3a), it is apparent that the principal reason for this discrepancy is the weak nocturnal respiration activity simulated by the corresponding flux parameterization. Thus, the nocturnal respiration is not sufficiently intense to replenish the CO_2 assimilated during the previous day.

Figures 4c and 4d show profiles for 1300 UTC (0900 LT) on the 14th and 1400 UTC (1000 LT) on the 17th July, typical of the morning periods. Both observed profiles show near-surface values higher than in the free atmosphere, where CO_2 levels can reach 390 ppmv, resulting from nocturnal respiration and weak turbulent mixing. The results of the CO_2[1] tracer are markeably superior to those of the CO_2[5] tracer and show good agreement with the observations. Again, the performance of the CO_2[5] simulation is compromised by the low prescribed nocturnal respiratory activity. In general, it can be concluded that the CO_2[1] tracer was able to reproduce in a satisfactory way the diurnal evolution of CO_2 in the bottom 3000 m of the atmosphere above the sampling area of the instrumented aircraft, mostly covered by forest.

The performance of the CO_2[1] tracer in simulating the diurnal CO_2 cycle above a spatial domain covering the majority of the Amazon is shown in Figure 5. A spatial average is calculated of the simulated CO_2 concentrations in the lower troposphere between longitudes 60ºW and 48ºW and latitudes 6ºS and 4ºN. Four average profiles are shown, corresponding to 1000, 1400, 1800 and 2200 UTC on July 11. These times are representative of how respiration, assimilation, and turbulent transport modulate the CO_2 profile throughout the day.

In the profile at 1000 UTC (0600 LT), an accumulation of CO_2 is observed near the surface, with average values on

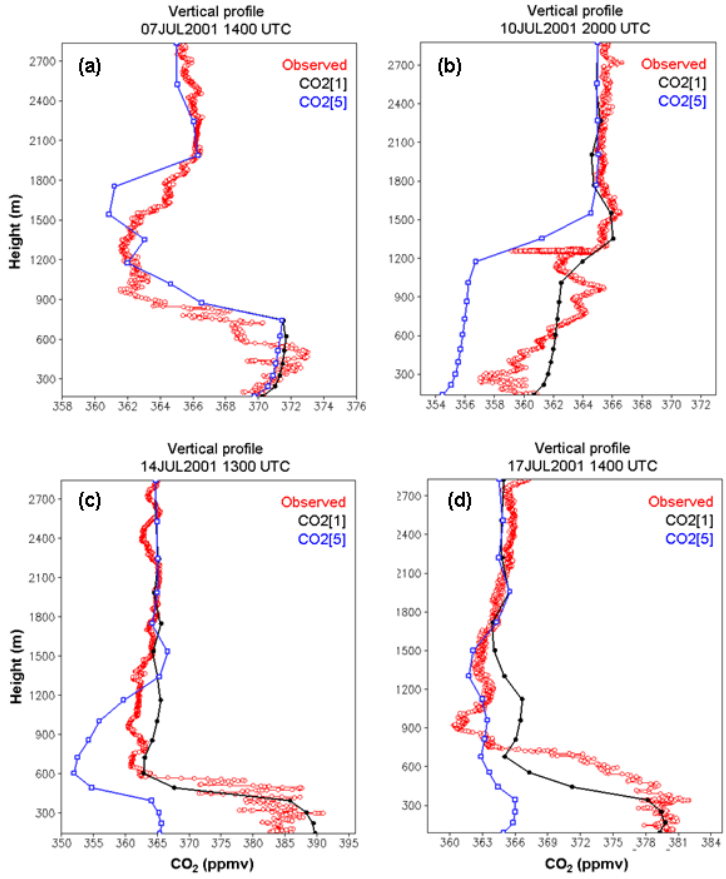

Figure 4 - CO2 profiles observed from aircraft measurements, compared with two tracers with two different flux parameterizations, averaged over a sampling area between longitudes 60º5'W and 59º5'W and latitudes 3º3'S and 2º3'S.

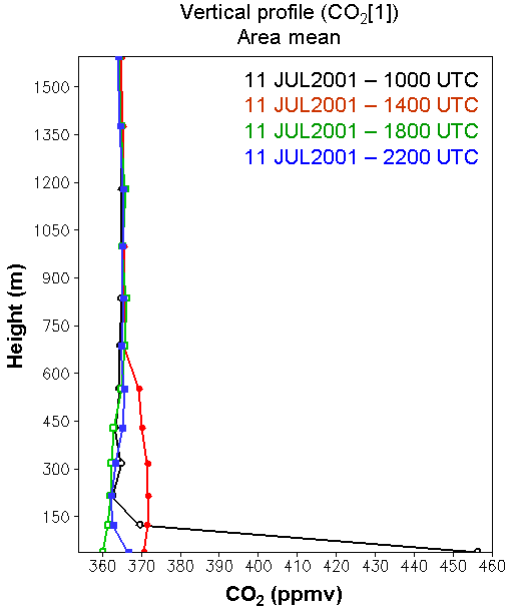

Figure 5 - Diurnal variation in CO2 in the lower troposphere, averaged over an area between longitudes 60ºW e 48ºW and latitudes 6ºS e 4ºN.

the order of 450 ppmv, caused by continuous respiration by the vegetation and soil during the night and low-level trapping of CO_2 due to the nocturnal atmospheric stability. At 1400 UTC (1000 LT) a shallow mixing layer has already formed with a depth of approximately 700 meters, with CO_2 concentrations slightly above 370 ppm due to turbulent transport that mixes the near-surface CO_2–rich layers with the relatively CO_2-poor layers above. Lower values are noted near the surface, indicating the occurrence of assimilation by vegetation. At 1800 UTC (1400 LT), there is a CO_2 deficit on the order of 6 ppm in the mixing layer relative to the free troposphere, due to the forest's photosynthetic activity. At 2200 UTC (1800 LT) the nighttime accumulation cycle of CO_2 has already started. From this analysis, it is concluded that the model was capable of correctly simulating the CO_2 cycle in the lower troposphere on a regional scale. Discussion of the role of convective systems follows.

With the objective of demonstrating the role of each transport process in the vertical CO_2 distribution, diverse tracers are utilized in accordance with Table 2. These different tracers are shown in Figure 6, principally to elucidate the rectifier effect. This effect, as previously defined, removes low-level concentrations of CO_2 and transports CO_2 to the

upper levels of the atmosphere. The values in the figure refer to a horizontal average of all grid points over the Amazon basin, with tropical forest as the dominant vegetation type. Analyzing the vertical profiles up to a height of 16 km, notable differences can be observed amongst the profiles. As previously defined, the tracers CO_2[1] through CO_2[4] use the parameterization obtained from the correlation between R_{net} and the CO_2 flux as a source/sink term. The CO_2[5] tracer uses the cosinusoidal parameterization. Spatially averaged profiles are shown for 1200 through 2200 UTC on July 11. For 1200 UTC (Figure 6a), a greater accumulation of CO_2 is noted in early morning, while at 2200 UTC (Figure 6b), a deficit is observed.

Analyzing each tracer with respect to its different characteristics, the contribution of each term in the transport equation to the atmospheric CO_2 distribution can be inferred. The CO_2[1] tracer, in accordance with Table 2, includes all terms from the transport equation, thus being the most realistic tracer for the simulation of CO_2 transport. The simplest case is the CO_2[4] tracer, which is transported only by mean wind and by turbulence in the PBL. As a result, this tracer shows a distinct profile shape in relation to the others. In this case, as would be expected, the free troposphere shows no variation in the tracer concentration. In the PBL, CO_2[4] has the highest CO_2 values due to the absence of convective transport mechanisms. The CO_2[3] tracer includes transport by shallow cumulus which impacts only the fists 4000 m, as seen previously. The CO_2[2] tracer includes the deep convective transport term and simulates the rectifier effect, which transports air masses with low CO_2 concentrations from the PBL to the high troposphere. Note that the CO_2[5] tracer, because it exhibits the greatest CO_2 deficit in the PBL, produces very distinct profiles due to the rectifier effect.

Figure 7 shows the rectifier effect on a horizontal level above the Amazon basin at an altitude of 14 km, corresponding to the approximate height where the maximum mass detrainment by convective systems occurs, as indicated in Figure 6. Figure 7 contains four subplots corresponding to 1700, 1900, 2100 and 2300 UTC on July 18, 2001. Three fields are shown: (1) horizontal wind streamlines, (2) contours of the hourly accumulation of convective precipitation (mm), in order to demarcate where convective systems are occurring, and (3) CO_2

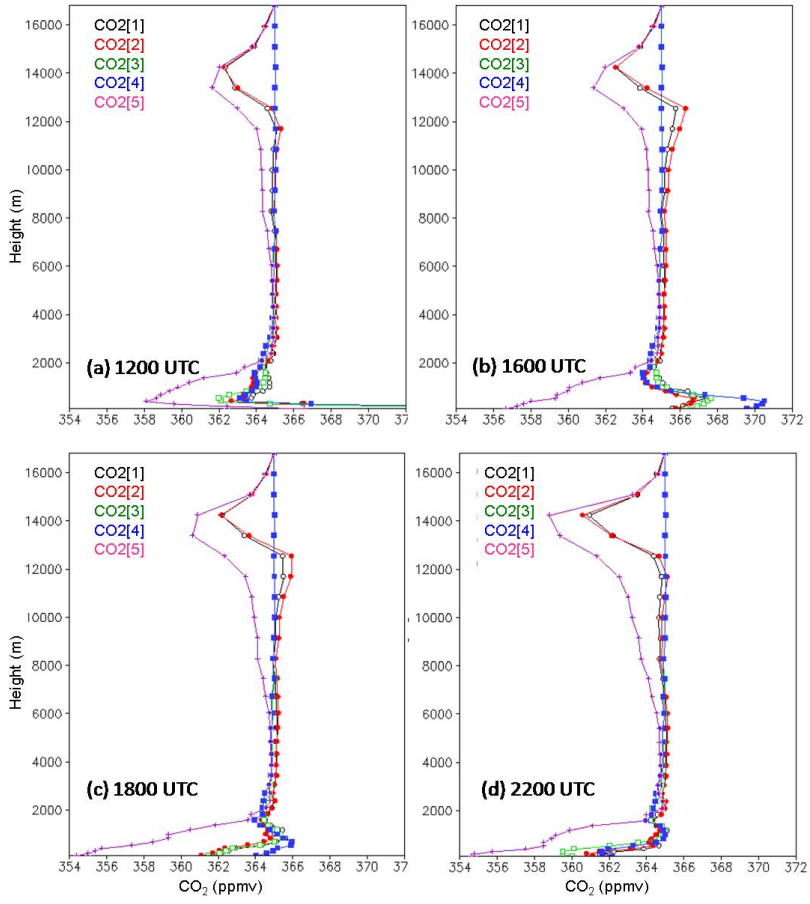

Figure 6 - Daily variation in CO2 concentration for different tracers, averaged over an area between longitudes 68ºW and 48ºW and latitudes 6ºS and 4ºN.

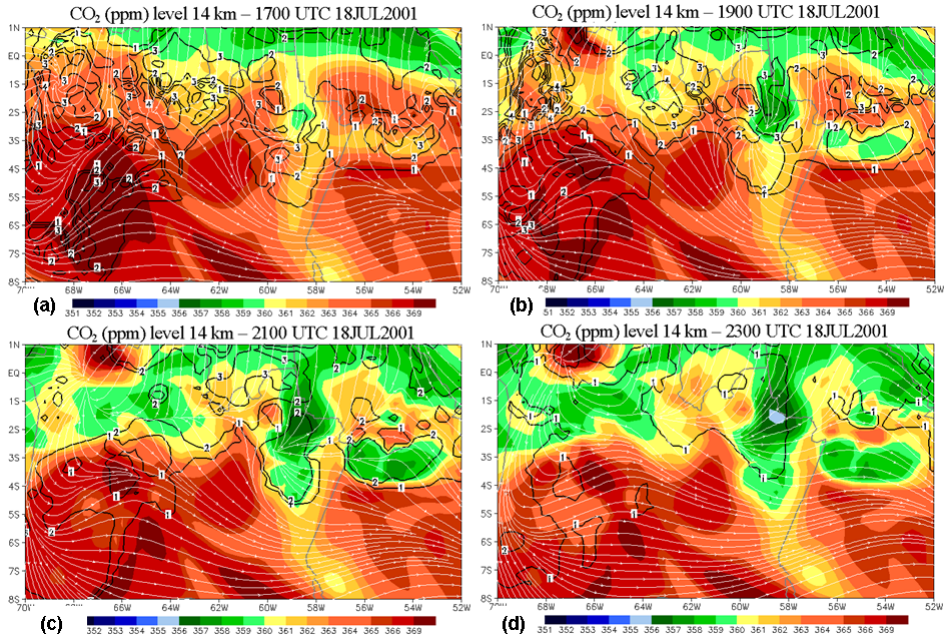

Figure 7 - Time evolution of CO2 concentration (shaded) for the tracer CO2[1] at an altitude of 14 km, streamlines (white), and hourly accumulated convective precipitation (contours in black, mm), between 1700 UTC and 2300 UTC on July 18, 2001.

concentration in ppmv for the tracer CO_2[1]. Observe that not all convective systems remove mass at this level, as there are systems with cloud tops below 14 km. The divergence of wind may be used to indicate the convective regions that detrain mass in this level. In this case, mostly of these areas are located at north of 4 S. In this region, the rectifier effect is significantly notable, with air masses containing CO_2 concentrations up to 10 ppm less than the background. It is also noted that due to the cumulative effect of assimilation by the forest, the CO_2 deficit intensifies throughout the afternoon, with the minimum CO_2 concentrations in the PBL in late afternoon.

An interesting discussion is raised from Figure 8, which includes four subplots over time of the vertical profile of the difference between the concentrations of the tracers CO_2[3] and CO_2[4] at latitude 3 S. As previously defined, the transport of CO_2[3] differs from CO_2[4] by the inclusion of the term associated with shallow convection, where CO_2[4] includes only advection by mean wind and turbulent transport in the PBL. Thus, this figure shows the net effect of these convective systems on the vertical distribution of CO_2. Analyzing the morning period between 1200 and 1400 UTC (subplots a and b), an enrichment of CO_2 is observed between 900 and 2000 meters of altitude. However, in the afternoon period between 1600 and 1800 UTC (subplots c and d), a depletion of CO_2 is observed in regions of active convection. This is explained by the fact that during the morning, shallow convection transports from the PBL air masses enriched with CO_2 by nocturnal respiration, and during the afternoon, air masses with a CO_2 deficit caused by the photosynthetic activity of the forest. Therefore, shallow convection can cause enrichment or depletion of CO_2 in the free troposphere, depending on the existing synchronism between shallow convection and the accumulated effect of the net CO_2 exchange between the forest and the surface boundary layer. The same feature can be described for deep convection. Since continental convection is strongly coupled to surface and boundary-layer processes, its typically observed diurnal cycle consists of the development of shallow cumulus in early morning and the transition to precipitating deep convection occurring in the afternoon. However, models typically simulate the onset of convective precipitation hours before it occurs in nature. This behavior has been verified, for example, in the model of the European Centre for Medium-Range Weather Forecasts, ECMWF (Betts and Jakob, 2002). This typical behavior of atmospheric models generates negative impacts not only in weather forecasting (for example, the temporal occurrence of rainfall and the maximum temperatures), but also to the atmospheric carbon budget estimation. Thus, the issue of correctly modeling the diurnal cycle of continental convection is also essential for studies of CO_2 budgets and its export from the Amazon by convective systems

4. CONCLUSIONS

In general, the transport model satisfactorily reproduced the general characteristics of the diurnal cycle of CO_2 in the PBL, and also its transport to the free troposphere by moist

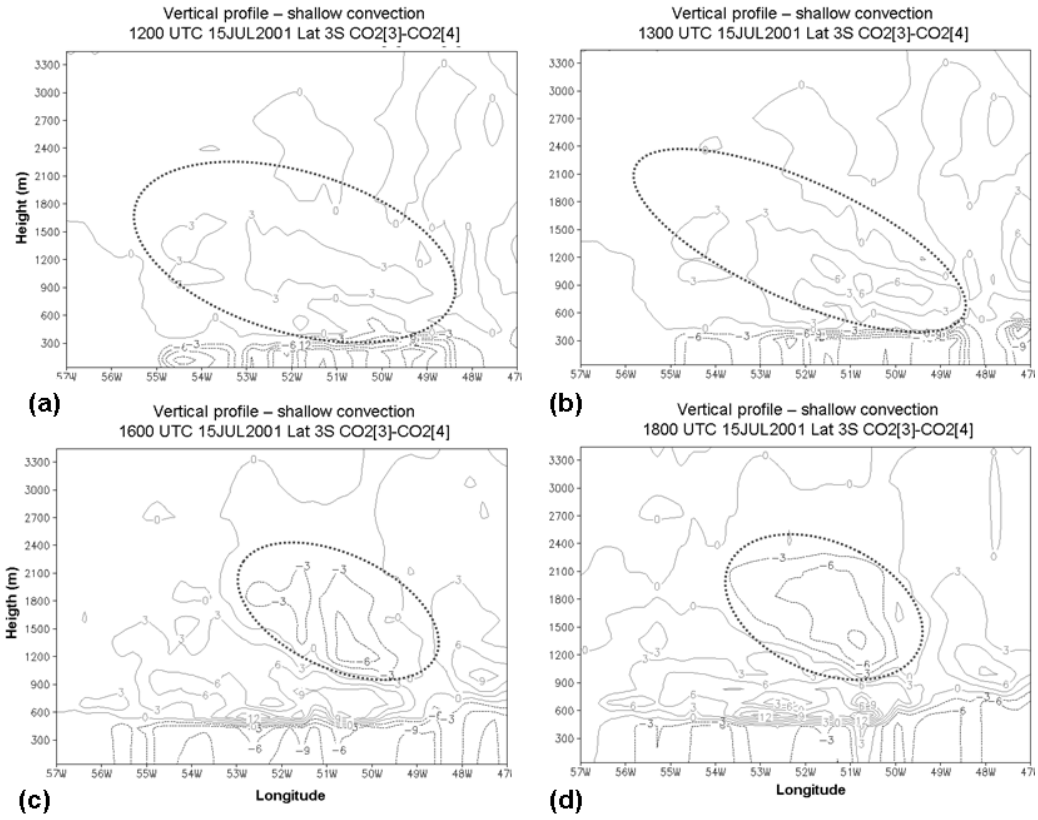

Figure 8 - Difference between the tracers CO2[3] and CO2[4], where the blue lines indicate the role of shallow convection when it is active in the morning (1200 and 1300 UTC) over a PBL still rich in CO2. Green lines show the rectifier effect of shallow convection when this occurs in the afternoon (1600 and 1800 UTC).

convective systems. Since the respiration of plants and soil occurs continuously and the assimilation of carbon takes place only during the day, there is a net emission of CO_2 to the atmosphere during the night. However, due to the nighttime atmospheric stability, the CO_2 stays confined near the surface, resulting in high CO_2 concentrations relative to the free troposphere in the early morning. During the day, assimilation by photosynthetic activity and the development of the mixing layer contribute to a gradual decrease of CO_2 inside the PBL. During sunny afternoons, a CO_2 deficit will exist inside the PBL relative to the free troposphere, and with the formation of deep convective systems, updrafts will transport these air masses to the upper troposphere, producing the so-called rectifier effect. In the case of shallow convection, which typically precedes deep convection, relatively low concentrations of CO_2 will be transported from the PBL to the low troposphere. However, in the early morning, the rectifier effect does not occur because the assimilation of CO_2 by the forest is still incipient, and thus shallow clouds transport high concentrations of carbon from the PBL to higher levels.

A relevant issue raised in this work is the relationship of modeling of the atmospheric carbon budget with modeling of the diurnal cycle of continental convection. The extreme diurnal variability of the CO_2 concentration in the PBL (accumulation at night and deficit during the day, relative to the troposphere) causes the transport by shallow or deep convective system to be strongly dependent on the time of day being simulated. Thus, accurate modeling of the diurnal cycle is not only important for improving the quality of forecasting, but also for calculating the carbon budget at regional and global scales.

5. ACKNOWLEDGEMENTS

The authors thank the program CLAIRE-LBA and Harvard University for the data used in this study. This study was funded by CNPq (master's fellowship) and FAPESP (2001/07874-9 e 2001/05025-4).

6. REFERENCES

ANDREAE, M. O., BROWELL, E. V., GARSTANG, M., GREGORY, G. L., HARRISS, R. C., HILL, G. F., JACOB,

D. J., PEREIRA, M. C., SACHE, G. W., SETZER, A. W., SILVA DIAS, P. L., TALBOT, R. W., TORRES, A. L; WOFSY, S. C. **Biomass-burning emissions and associated haze layers over Amazonia,** J. Geophys. Res., v. 93, no D2, p. 1509-1527, Fev. 1988.

BETTS, A.; C. JAKOB. **Evaluation of the diurnal cycle of precipitation, surface thermodynamics, and surface fluxes in the ECMWF model using LBA data**. J. Geophys. Res., V. 107, D20, doi: 10.1029/2001JD0000427, 2002.

CHEN, C.; W.R. COTTON. **The physics of the marine stratocumulus- capped mixed layer**, J. Atmos. Sci., v. 44, p. 2951-2977, 1987.

FREITAS, S. R., K. LONGO, M. SILVA DIAS, P. SILVA DIAS, R. CHATFIELD, E. PRINS, P. ARTAXO, G. GRELL; F. RECUERO. **Monitoring the transport of biomass burning emissions in South America**. Environmental Fluid Mechanics, DOI: 10.1007/s10652-005-0243-7, v. 5 n. 1-2, p. 135 – 167, 2005.

FREITAS, S. R., LONGO, K. M., SILVA DIAS, M. A. F., CHATFIELD, R., SILVA DIAS, P., ARTAXO, P., ANDREAE, M. O., GRELL, G., RODRIGUES, L. F., FAZENDA, A.; PANETTA, J. **The Coupled Aerosol and Tracer Transport model to the Brazilian developments on the Regional Atmospheric Modeling System (CATT-BRAMS) – Part 1: Model description and evaluation**, Atmos. Chem. Phys., v. 9, p. 2843-2861, 2009.

GEVAERD, R. E; S. R. FREITAS. **Estimativa operacional da umidade do solo para iniciação de modelos de previsão numérica da atmosfera. Parte I: Descrição da metodologia e validação**. Revista Brasileira de Meteorologia, v. 21, n. 3a, p. 59-73, 2006.

GRELL, G. A. **Prognostic evaluation of assumptions used by cumulus parameterizations**. Mon. Wea. Rev., v. 121, n. 3, p. 764-787, 1993.

GRELL, G. A.; D. DEVENYI. **A generalized approach to parameterizing convection combining ensemble and data assimilation techniques.** Geophysical Research Letters, v.. 29, n. 14, 2002.

HOUGHTON, R. A. **The Global Effects of Tropical Deforestation**. Environ. Sci. Technol., v. 24, n.. 4, p. 414-422, 1990

HERRMANN, V. **Balanço de CO2 na Atmosfera da Bacia Amazônica: O Papel dos Sistemas Convectivos**. 2004. Dissertação (Mestrado em Ciências Atmosféricas, in portuguese), IAG, Univeridade de São Paul, São Paulo, 2004.

LLOYD, J., O. KOLLE, H. FRITSCH, S. R. FREITAS, M. A. F. SILVA DIAS, P. ARTAXO, A. D. NOBRE, A. C. DE ARAJO, B. KRUIJT, L. SOGACHEVA, G. FISCH, A. THIELMANN, U. KUHN; M. O. ANDREAE. **An airborne regional carbon balance for Central Amazonia**, Biogeosciences, v. 4, p. 759-768, 2007.

LU, L., DENNING, A. S., DA SILVA-DIAS, M., DA SILVA-DIAS, P., LONGO, M., FREITAS; S. R. SAATCHI, S. **Mesoscale circulations and atmospheric CO variations in the Tapajós Region, Pará, Brazil.** Journal of Geophysical Research, v. 110, p. D21102, 2005.

MALHI, Y., NOBRE, A. D., GRACE, J., KRUIJT, B., PEREIRA, M. G. P., CULF, A.; SCOTT, S. **Carbon dioxide transfer over a central Amazonian rain forest,** J. Geophys. Res. v. 103, n. D24, 31, p. 593-3, 612, 1998.

MELLOR, G.; YAMADA, T. **A hierarchy of turbulence closure models for planetary boundary layers,** J. Atmos. Sci. v. 31, n. 1791-1806, 1974.

MIRANDA, A. C., MIRANDA, H. S., LLOYD, J., GRACE, J., MCINTYRE, J. A., MEIR, P., RIGGAN, P., LOCKWOOD, R; BRASS, J. **Carbon dioxide fluxes over a cerrado sensu stricto in central Brazil. Amazonian deforestation and climate**, eds. J. C. H. Gash, Nobre, C. A., Roberts, J. M., Roberts and Victoria. John Wiley and Sons, Chichester, UK, p. 353-363, 1996.

SALESKA, S. R., MILLER, S. D., MATROSS, D.M., GOULDEN, M. L., WOFSY, S. C., ROCHA, H. R., CAMARGO, P. B., CRILL, P., DAUBE, B. C., FREITAS, H. C., HUTYRA, L., KELLER, M., KIRCHHOFF, V., MENTON, M., MUNGER, E. H., PYLE, E. H., RICE, A. H.; SILVA, H. **Carbon in Amazon Forest: Unexpected Seasonal Fluxes and Disturbance-Induced Losses**. Science, v. 302, p. 1554-1557, 2003.

SESTINI, M., REIMER, E., VALERIANO, D., ALVALÁ, R., MELLO, E., CHAN, C.; NOBRE, C. **Mapa de cobertura da terra da Amazônia legal para uso em modelos meteorológicos,** Anais XI Simpósio Brasileiro de Sensoriamento Remoto, p. 2901-2906, 2003.

SMAGORINSKY, J. **General circulation experiments with the primitive equations. Part I: The basic experiment**, Mon. Wea. Rev. 91, 99-164, 1963.

TAKAHASHI, T., WANNINKHOF, R. H., FEELY, R. A., WEISS, R. F., CHIPMAN, D. W., BATES, N., OLAFSSON, J., SABINE, C.; SUTHERLAND, S. C. **Net sea-air CO_2 flux over the global oceans: An improved estimate based on the sea-air pCO_2 difference.** Proceedings of the 2nd International Symposium CO_2 in the Oceans, Tsukuba, Janeiro de 1999.

TAYLOR, J. A.; LLOYD, J. **Soucers and sinks of atmospheric CO_2,** Aust. J. Bot., v. 40,p. 407-418, 1992.

TREMBACK, C., POWELL, J., COTTON, W.; PIELKE, R. **The forward in time upstream advection scheme: Extension to higher orders**, Mon. Wea. Rev. v. 115, p. 540-555, 1987.

WALKO, R., BAND, L., BARON, J., KITTEL, F., LAMMERS, R., LEE, T., OJIMA, D., PIELKE, R., TAYLOR, C., TAGUE, C., TREMBACK, C., VIDALE, P. **Coupled atmosphere-biophysics-hydrology models for environmental modeling,** J. Appl. Meteorol., v. 39, n. 6, p. 931-944, 2000.

WHITTAKER, R. H., LIKENS, G. E. **The biosphere and man, in primary productivity of the biosphere**, p. 305-328, Springer-Verlag, New York, 1975.